

# Demonstration of Technologies for Autonomous Micro-Satellite Assembly

William A. Bezouska<sup>1</sup>, Michael R. Aherne<sup>2</sup>, J. Tim Barrett<sup>3</sup>, Steve J. Schultz<sup>4</sup>

**Next generation space structures need on-orbit assembly due to volume limitations on launch vehicles. Many assembly strategies exist; one such is the notion of autonomous Micro-satellites used to grab, transport, and assemble individual structures. The University of Southern California's (USC) new Micro-satellite Dynamic Test Facility (MDTF) is demonstrating full scale assembly techniques using independent and autonomous micro-satellite prototypes with five foot passive beams. All testing is performed on a frictionless 3DOF hyper flat surface platen, with both inertial and relative positioning systems. The micro-satellites are independent spacecraft prototypes capable of attitude control that provide a test bed for space based operations. Designed to reduce cost and maximize simplicity, micro-satellites have been used to test spacecraft maneuvers at the MDTF. Their wireless communication ability has been used to produce teams for formation flying or collaborative operations. USC's current research focused upon the technologies necessary for one element of autonomous assembly is showcased here with beam assembly.**

## I. Introduction

The challenge of on-orbit space assembly can be divided into many characteristic elements. An assembly mission involves a host of complex problems, including accurate localization (both of oneself and the object(s) one needs to assemble), the act of docking, post-docking control algorithms, and decentralized collaboration. Other universities and programs have made significant strides in addressing these individual problems<sup>1,2,3,4</sup>, and have demonstrated various facets of their solutions at specialized facilities<sup>5</sup>, the KC-135 Research Airplane<sup>6</sup>, and the International Space Station<sup>7</sup>. While solutions to specific challenges have been emerging from these efforts, it is leading to a full systems architecture addressing both technology and autonomy in a consolidated test bed to prove actual full scale on-orbit assembly techniques. This is the goal for the MDTF.

The Information Sciences Institute (ISI) and the Space Engineering Research Center (SERC) at the University of Southern California (USC) recently completed the installation of a new facility, created to enable real-world testing of full-scale rendezvous and proximity operations. This location, known as the Micro-satellite Dynamic Test Facility (MDTF), allows researchers to demonstrate autonomous satellite behaviors such as formation flying or autonomous rendezvous in an affordable environment. The enabling components of the MDTF are the large precision flat floor and an initial fleet of five autonomous micro-satellite prototypes. Ongoing research at this facility is exploring the various challenges and difficulties associated with space assembly. In this paper, we will give an overview of the critical MDTF components, a review of the global space assembly architecture, specific research paths that our facility is supporting, our current work on a relative position sensor suite, and the future work in this area.

---

<sup>1</sup> Graduate Student, USC ASTE, Guidance, Navigation, and Control, Space Engineering Research Center

<sup>2</sup> Graduate Student, USC ASTE, Guidance, Navigation, and Control, Space Engineering Research Center

<sup>3</sup> Senior Electrical Engineer, USC/ISI

<sup>4</sup> Mechanical Design Engineer, USC/ISI

## II. Micro-satellite Dynamic Test Facility (MDTF)

USC's MDTF was developed to serve as a full-scale autonomous rendezvous and proximity operations research platform<sup>8</sup>. Located in Southern California, the facility allows multiple heterogeneous satellites to practice complex spacecraft missions while floating on air bearings in a near-frictionless environment (Fig. 1).

### A. Precision Flat Floor

To simulate space operations, a precision flat floor at was installed in a shared facility. This 9.1m by 13.7m epoxy floor is flat to within 0.0005 inches in any 3m-radius section. This surface provides realistic, unconstrained motion in three degrees-of-freedom (DOF). Specifically an object on air bearings can move freely in two translational directions ( $x$  and  $y$ ) and one rotational direction ( $\psi$ ). The surface area is large enough to support multiple full-size vehicles simultaneously.

### B. Micro-satellite Prototypes

A foundation for the MDTF rendezvous and proximity operations testbed uses a set of micro-satellite prototype vehicles. Designed with interchangeable commercial off-the-shelf (COTS) components and some custom avionics, these vehicles provide a very low cost test bed for complex operations at the MDTF. Each vehicle contains a PID-based, waypoint-driven control system and can maneuver using cold gas thrusters. Onboard batteries, compressed air and a wireless access point allow the vehicles to operate untethered. A star-tracker-like system senses infrared emitters in the ceiling to provide position and rotation information, and the top of each vehicle serves as a payload space.

### C. Ground Control

A ground control station is able to command the vehicles over a private wireless network. Each vehicle can receive and respond to plain-text commands, using an application programming interface. Vehicle telemetry is received and displayed in a custom-made JAVA-based control program. The graphs and video telemetry are displayed at the ground station and can be projected onto a screen at the far end of the room.



**Figure 1. The Micro-satellite Dynamic Test Facility.** The four vehicles shown here are the micro-satellite prototypes. A portion of the ground control station is visible in the lower left.

## III. Space Assembly Architecture Overview

Future structures in space are likely to be very large and complex (ie solar power system, large apertures, etc). It is conceivable that there would be from hundreds to thousands of components or elements, all individually placed on orbit (in groups as example) and needing assembly. This scope of assembly may be too large for astronauts due to both safety and logistics, and ultimately cost. Thus, one concept for creating these very large structures is through use of autonomous robotic assembly<sup>9</sup>.

This approach will require a very robust research and development program that would benefit from low cost Earth based testing, and by multiple groups and organizations concentrating on various key elements. The notion of flying and controlling hundreds to

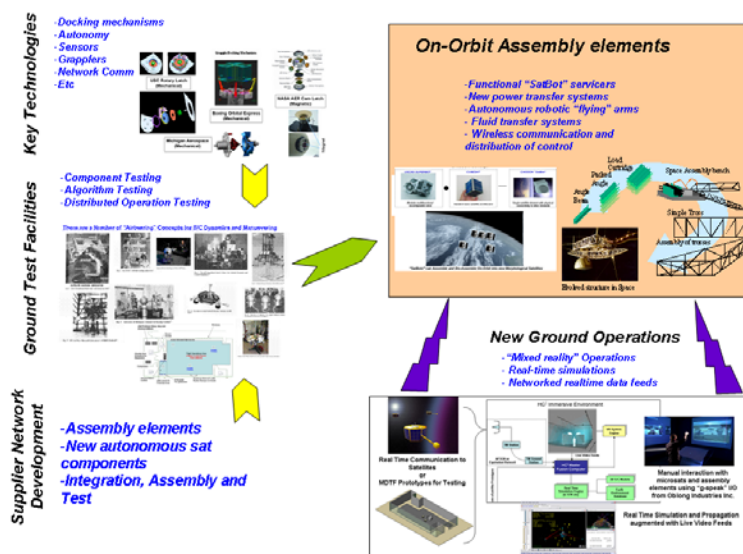


**Figure 2. System level architecture for on-orbit autonomous space assembly**

thousands of elements on orbit brings out a myriad of technically challenging issues that have to be resolved and worked on.

To achieve a successful on orbit assembly effort, the problem requires a system level architecture view which includes such elements as ground development, testing, manufacturing, supplier development, launch and on orbit operations needs to be considered and thought of. Figure 2 shows a notional system level architecture that USC is in process of developing for autonomous on orbit assembly elements, infrastructure, testing and ground operations<sup>10</sup>.

#### IV. Initial Research Paths for Autonomous Space Assembly

The MDTF has created a foundation for full-scale space-based assembly research in four key areas, and USC has begun to build upon this foundation. Each area and the current state of USC research is summarized below.

##### A. Connection Methods

Many types of connections exist, and they can be loosely categorized in a hierarchy as shown in Fig. 3. In the figure, structural connections refer to a rigid physical interfacing between objects; electrical and consumables refer to the additional connections required to transfer data, power, or propellant. “Cooperative/Uncooperative” refers to whether both of the objects have specialized docking hardware, and “Active/Passive” refers to whether this hardware can be actuated open and closed.

USC is currently performing research on docking with uncontrolled, free-floating beams. The beams are fitted with a simple docking mechanism, and a targeting pattern. The research has two focuses: (1) to demonstrate beam assembly techniques and (2) to demonstrate cooperative sensor docking techniques with a passive uncooperative receiving mechanism.

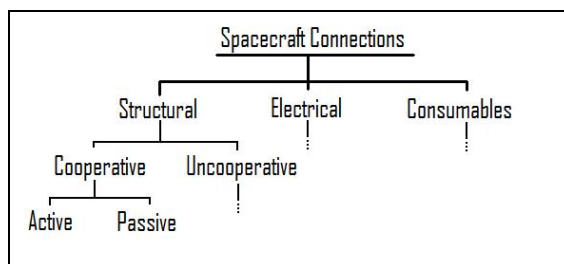


**Figure 3. Example Spacecraft Connection Hierarchy**

##### B. Object Localization

The position and attitude of all objects involved in space assembly must be known during rendezvous and proximity operations. This includes satellite teams, truss components, and any other objects that may affect the mission. The accuracy requirement for this localization data may change as operations progress. For example, attitude knowledge at a range of 1km is not crucial. However, the attitude accuracy requirement at 1m may be  $\pm 1$  degree. To achieve this sliding requirement, staged sensors are being created, starting with a close-range sensor suite to allow localization at ranges between 0 to 5m.

##### C. Active and Passive Spacecraft Assembly Techniques

Once relative space object pose is known and a method to connect to the space object exists, an intelligent system must execute both docking and assembly maneuvers. In some instances this includes an interaction between a passive beam and an active assembler satellite. In other cases, two active satellites, each of which is attached to a passive beam, must collaborate and connect the beams tip to tip. It is important to maintain collision avoidance and fault detection during these operations.

Some specific research areas include exploring the effects of plume impingement on tip-to-tip beam connections, investigating trajectory planning methods for aligning beams with an assembler micro-satellite, understanding optimized mechanical and electrical beam tip to tip connectivity and latching mechanisms, and strategies for maintaining a partial structure during assembly and reconfiguration after assembly.

##### D. Decentralized and Distributed Operations

By creating identical satellites and enabling decentralized operation, the space assembly system can increase both efficiency and robustness. If all satellites are identical, efficiencies are available during satellite production on the ground. If one satellite fails on orbit, any team member can replace it. A distributed architecture does not require commands from the ground segment, nor is a large primary satellite needed on orbit. Individual satellites can undertake master roles, or tasks may be automatically acquired by satellite team members. Specific examples of this research include distributed communications, simultaneous localization and mapping (SLAM), task assignment, fault recovery, and advanced distributed formation flight and obstacle avoidance algorithm development.

USC is currently exploring methods of decentralized collision avoidance, inspired by behavior-based control algorithms<sup>11</sup>.

## V. Current Work -- Relative Sensor Suite

In the final stages of docking, vehicles can no longer rely on inertial measurements, as the tolerances needed greatly exceed the capabilities of most inertial localization systems. To perform research in this area, USC has created an inexpensive sensor suite to achieve sufficient attitude and position knowledge for docking. This suite aims to provide continuous state measurements of a known space object between distances of 0 to 5 meters. The objective is met using an actuated CMOS camera and static infrared (IR) rangefinders. These COTS sensors are mounted as shown in Fig. 4. The components and algorithms of this sensor suite are described in detail below.

### A. CMOS Camera

The camera is a 1/5" CMOS 1.3 megapixel camera which provides 640x480 resolution images at 30 frames per second (fps). The camera is mounted to a pan and tilt servo kit from Trossen Robotics<sup>TM</sup>. The servos are connected to an 8-motor Phidget<sup>TM</sup> controller. Both the Phidget controller and camera connect to a host laptop via USB.

The gimballed movement of the pan and tilt servos allows a theoretical maximum of  $4\pi$  steradians in the viewing field. Because the system is implemented on a flat floor at the MDTF, the tilt servo is locked at 0 degrees. Even with obstructions, the camera can accurately track objects in a 180 degree azimuth field of view. This compares to a fixed mount field of view of 40 degrees.

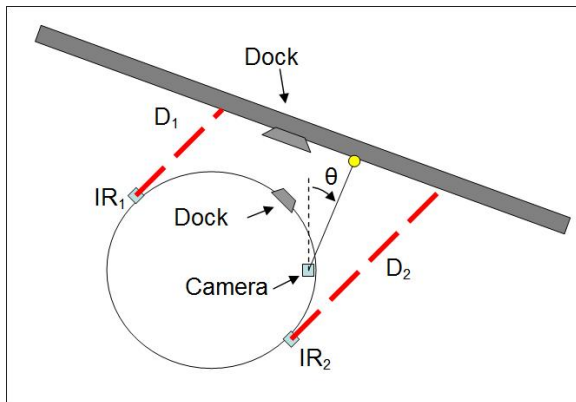


Figure 4. Sensor Mounting Location

### B. IR Rangefinders

The Relative Sensor Suite includes two side-mounted Sharp Infrared sensors (GP2Y0A02YK). These provide accurate distance measurements in a range of 20cm to 150cm from a given object. The mounting location ensures that a docked beam resides at the minimum readable range. The sensor accuracy increases as the distance to object decreases. This is advantageous for RPO because the accuracy requirement increases as the distance between two docking objects decreases. These sensors are used during short pose estimation.

### C. Space Object Fiducials

The objective of the fiducial system is to provide simple and low cost visual markings for the satellite vision system to compute relative vehicle pose and location.

The current fiducial system installed on construction beams at MDTF is shown in Fig. 5. The configuration, consisting of three colored dots, allows computer vision algorithms to isolate and analyze the pattern. The pink

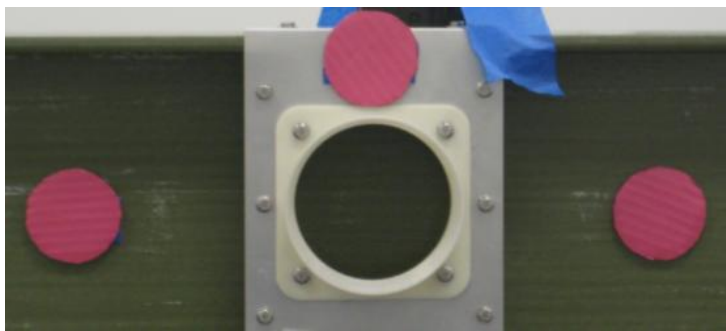


Figure 5. Fiducial Mounted on Beam.

color contrasts existing colors in the facility, thus making segmentation easier. However, any contrasting color should produce similar results. The right and left dots are co-planar in the vertical plane while the center dot is 5cm out of plane. Their relative positions may be arbitrary, but must be known for pose and location estimations. All three dots must not be in the same image plane. The computer vision software tracks the position of the center of each dot. Therefore, the circular shape was chosen to make centroiding more accurate and repeatable.

During short range sensing, an additional fiducial (not shown) is used by the computer vision system to aid in pose determination. It is yellow to contrast with the existing markings as well as the MDTF environment. A smaller diameter has been chosen so that during short range vision, a similar amount of pixels are required to represent the dot as during long range sensing using the pink fiducials.

#### D. Computer Vision Software

The relative sensing system leverages the Open Computer Vision Library (OpenCV). This open source software library performs core image manipulation and analysis. The process starts with OpenCV identifying the location of each dot in image coordinates. These coordinates are placed into a pose estimation function, producing a real world attitude and vector to the object. All image processing and associated pose estimation operates on a separate computer which has been placed in the payload location of the micro-satellite. At specified intervals the computer vision software sends a pose update packet to the satellite flight processor via wireless IP. The current sensor update rate is 1 Hz. This rate is caused primarily from the amount of averaging involved. However, depending on camera frames-per-second (fps) and computer processing power, future implementations may be possible at 10Hz.

The process of identifying a fiducial is separated into 3 basic steps as described below.

##### 1. Color Segmentation

After receiving an image from the webcam, the colorspace of the image is transformed from Red-Green-Blue (RGB) to Hue-Saturation-Value (HSV). The HSV format is more intuitive and provides an easier means of segmenting colors. To separate an individual color from an image, the OpenCV function `cvInRangeS()` is used. This function scans all the pixels in an image, zeroing out any that do not fall within specified ranges for hue, saturation, and value. Hues range from 0 to 180, roughly following the colors of the rainbow (ROY-G-BIV). Saturation is a measure of the intensity of the color, on a scale from grey (0) to full color (255). Value is a measure of the brightness or “shininess” of a color, ranging from black (0) to white (255). To extract the pink dots, we use an inclusive hue range from 160 to 6 (passing through 0), a saturation range of 50 to 255, and a value range of 100 to 255. These values were experimentally determined. The effect of this segmentation is seen in the top right portion of Fig. 6. It should be noted that this process changes the color depth of the image from 3 channels (HSV) to 1 channel (Grayscale). At this color depth, each pixel is assigned a value from black (0) through gray to white (255).

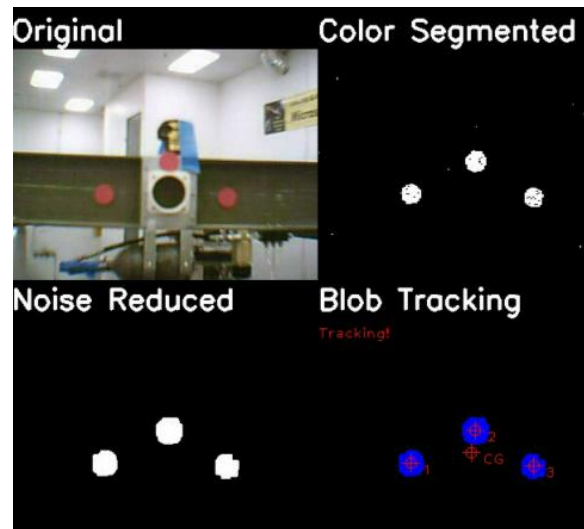


Figure 6. Image Processing Steps.

##### 2. Noise Reduction

Once the colors have been isolated, the resulting grayscale image goes through a noise reduction process. We perform a Gaussian smoothing on the image using the OpenCV function `cvSmooth()`. This has the effect of making the image “fuzzy.” Specks of noise are dithered from white to grey. We take advantage of this effect by performing a threshold using `cvThreshold()`. Any pixel grayer than 230 is rejected. Lastly, to fill in the gaps within each dot, we use the function `cvDilate()`. This function effectively “grows” the remaining white spaces, resulting in the image in the lower left of Fig. 6.

##### 3. Blob Detection

Blob detection is performed using an auxiliary library designed for OpenCV called `cvBlobsLib`. This library performs 8-connected component extraction on binary images. Detected blobs are put through a rigorous sequence of validation checks which exploit the known geometry of the fiducial. This ensures that even in the presence of significant noise (for example, a person with a red shirt walking in the background), only the 3 blobs which produce the expected triangular shape are retained.



## E. Long Range Pose Estimation

After being extracted from the image, the coordinates of all three dots are fed into a pose estimation algorithm (see Eq. 1). The algorithm requires knowledge of the spatial relationship of the three dots in real world coordinates. Specifically, the distance between the outer dots and the center of the dock ( $c$ ) and the distance that the middle dot protrudes from the beam plane ( $a$ ) are required.

$$\psi = \tan^{-1} \left( \frac{-a \left( \frac{d_1}{d_2} - 1 \right)}{c \left( \frac{d_1}{d_2} + 1 \right)} \right) \quad (1)$$

$$y = \frac{320}{\tan(FOV)} \cdot \frac{c \cdot \cos(\psi)}{d_1 + d_2} \quad (2)$$

First, the relative rotation ( $\psi$ ) of the beam is computed. This relies on the ratio of distances between the three dots. Therefore, these distances do not need to be converted to real world units first. Second, the distance to object ( $y$ ) is computed by comparing the object size to the image FOV. It is assumed that the object is centered in the frame by the camera servo at all times. Therefore, we can combine these two computed values with the camera pan value to produce a relative position and attitude of the object in the satellite coordinate frame.

The algorithm was created using a weak perspective projection. (See Fig. 7). This assumption is valid for pose estimation when two conditions are present. First, the object must be “close” to the image center. Second, the object size must be “small” when compared to the distance from camera to object. The conditions for “closeness” or “smallness” are not computed analytically, but rather empirically during full system testing.

To achieve the second condition, the pan and tilt system centers the object within the image frame at all times. A software-based PID controller attempts to minimize the distance between the center of the camera image and the center of the object. To reduce the effect of PID settling time, pose estimates are averaged over a one second interval before being transmitted to the flight processor.

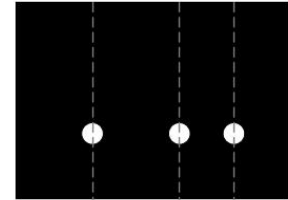
## F. Short Range Pose Estimation

The weak perspective projection assumption used for long range pose estimation is only valid when the object’s dimensions are small when compared to the distance to the object. As the satellite approaches the beam, this assumption begins to become invalid. At this point a short range sensor system is required. Refer to Fig. 4 above.

Two side mounted IR rangars are used to determine the distance to the beam as well as the rotation of the beam relative to the spacecraft. Because the beam is flat with low reflectivity, the IR rangars produce accurate results ( $d_1$  and  $d_2$ ). To determine the final dimension required for complete state knowledge, the camera tracks the single yellow fiducial marking. By returning the pan angle to that fiducial ( $\theta$ ), complete state estimation is possible. The algorithms used to determine pose using this set of data are shown in Eq. 3 through Eq. 5.

$$\psi = \tan^{-1} \left( \frac{d_1 - d_2}{a} \right) \quad (3)$$

Image Frame View



Top Down View

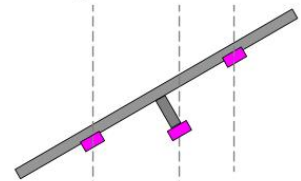


Figure 7. Long Range Pose Estimation

$$x = \left[ \frac{(d_2 - d_1)}{2} + d_1 \right] \cdot \cos(\psi) \quad (4)$$

$$y = \frac{x}{\tan\left(\frac{\pi}{2} + \psi - \theta\right)} \quad (5)$$

First, the relative rotation of the beam ( $\psi$ ) is computed using the difference between the IR ranger measurements. Next, the algorithm computes the relative position of the beam ( $x, y$ ) in a coordinate frame located at the camera. A simple coordinate transformation can move this frame to the satellite body coordinates.

### G. Six Degrees of Freedom (6DOF) Pose Estimation

The current sensing system at the MDTF determines beam attitude in one angular dimension ( $\psi$ ) and position in two linear dimensions ( $x$  and  $y$ ). This simplification has been performed because the flat floor allows operations on one plane. However, the system can be extended to compute both pose and position of space objects in a 6DOF environment.

To perform localization, the fiducial system must be upgraded to include four dots, all of which cannot be coplaner. The same process described above can be used to extract the centroid location of each dot or blob. Once the location, in image coordinates, of all the markings is found, a function called POSIT<sup>12</sup> can be used to determine the real world pose and location of the object.

Unfortunately, this method suffers from the same weak perspective restriction as above. Although POSIT can be used for long range sensing, a new approach will be required for short range 6DOF pose estimation.

### H. Preliminary results

#### a. Cost of systems

As an example of a university based approach to real-world problem solving, the total cost of the sensing system is shown in Table 1. This cost does not include the personal laptop used to run the image processing code.

**Table 1. Total Cost of the Relative Sensor Suite.**

Item	Cost	
Pixxo AW-I1130-BK Black Webcam	\$	14.99
SHARP IR (GP2Y0A02YK) (2 units)	\$	25.98
Pan and Tilt Kit with Servos	\$	28.45
Phidget 8-Motor Controller	\$	69.95
<b>Total</b>	<b>\$</b>	<b>139.37</b>

#### b. Relative sensor accuracy results.

Figure 8 shows the summary relative sensor results for accuracy.



**Figure 8. Long Range Pose Estimation**

## VI. Future Work - Autonomous Docking

### A. Latch Mechanism

The micro-satellites at the MDTF currently connect to each other using a simple latch mechanism as shown in Fig. 9. The mechanism is designed for zero-velocity docking. The capture vehicle is equipped with the male component which houses the actuated latching mechanism (see the leftmost vehicle in Fig. 1). The female receptacle is attached to the beam and has no moving parts (see Fig. 5). Before a docking sequence is begun, the solenoid is activated to open the latch. Once the male and female docking components are aligned, the solenoid is deactivated, rigidly capturing the beam.

USC has rapid-prototyped this design using a 3D printer. The rapid prototyping has allowed us to produce plastic latches quickly and efficiently. However, the use of plastic has some drawbacks. The activated solenoid produces a large amount of heat, and on one occasion has been able to melt the connection between itself and the latch. Future plans include collaborating with the other universities and research institutes that have various docking mechanisms for testing of both experimental and more mature latch designs that would lend themselves to autonomous assembly on orbit assembly systems.

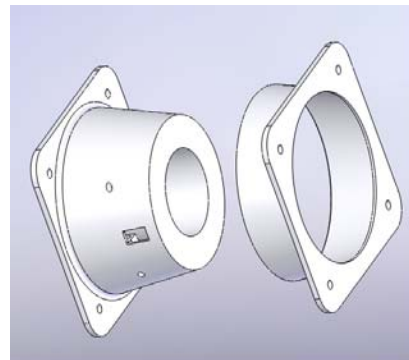


**Figure 9. Latch Mechanism.**

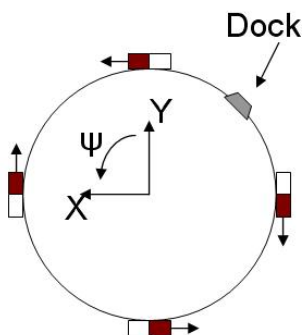


**Figure 10. Thruster Restrictions during docking maneuvers.**

### B. Docking Mode Thrusters

Thruster plume impingement has negatively affected docking performance in some cases. Specifically, as the micro-satellite approaches the beam, the cold gas thrusters tend to push the beam away from the satellite. As the satellite attempts to follow, the problem repeats and amplifies.

To prevent this, the thruster decision engine will be adjusted to include a docking mode. During normal mode, all thrusters are available for attitude and position control. However, when the spacecraft is within some region of the target, only certain thrusters will be used to produce the least impingement (see Fig. 10). This has the added benefit of reducing the resultant thrust along the docking vector thereby further slowing closing velocity per minimum impulse. Future work includes determining the size of this region, the resolution lost from a restricted thruster set, and looking

at additional thruster configurations (figure eight, bow-tie, etc).

### C. Trajectory Planning

Once the micro-satellite and beam are rigidly connected, the dynamics of the combined system are different from that of the micro-satellite alone. While we could analyze the system and hard-code a solution, this would be ignoring the larger issue. Assembly spacecraft will have to dock repeatedly with beams and structures of vastly different sizes and moments of inertia. With that in mind, USC is investigating generic motion algorithms that can be used to move a beam or structure regardless of size. Future work falls along three avenues. First, inspired by Cassini's on-board determination of mass properties<sup>13</sup>, we will attempt to make our micro-satellites derive the mass properties of the object to which they are docked. Then, we will develop generic guidance algorithms to allow the micro-satellites to control the motion of the combined system. Finally, we will experimentally determine when a micro-satellite should call for help from another micro-satellite instead of trying to move or rotate a structure by itself.

## VII. Conclusion

Continuing high launch mass cost, increasing complexity in micro/nano-satellite systems, and the ever expanding desire for greater expansion of mechanical and electrical systems on orbit will require forays into on orbit assembly.



The current field of on orbit autonomous assembly follows both small scale lab demo's, and use of the ISS both for demonstration regime and examination of assembly using combination of manned and robotic systems. There are many difficult and critical technical challenges required to solve before a fully autonomous system of micro/nano/pico-satellites can assemble completely autonomously a large scale space structure and system. USC's Micro-satellite Dynamic Test Facility (MDTF) is operational today and able to demonstrate in real-time multiple autonomous microsatellite prototypes in 3DOF for distributed and autonomous operations. USC believes this field of study is critical to the future expansion of larger elements and applications in space and is working to develop a system level architecture that utilizes the high number of technologies under development and proven by universities and institutes to-date.

## **VIII Acknowledgments**

The authors would like to thank Alejandro Fernandez, Allison Anderson and Kristina Rojdev for initial support on the API, and to the developers, contributors, and maintainers of OpenCV.

## **References**

- 
- <sup>1</sup> Schwartz, J.L., Peck, M.A., Hall, C.D., "Historical Review of Spacecraft Simulators." AAS 03-125.
  - <sup>2</sup> Ma, Ou and Martin, E., "Extending the Capability of Attitude Control Systems to Assist Satellite Docking Missions"
  - <sup>3</sup> Carrico, T., Langster, T., et al. "Proximity Operations for Space Situational Awareness : Spacecraft Closed-Loop Maneuvering Using Numerical Simulations and Fuzzy Logic." Advanced Maui Optical and Space Surveillance Technologies Conference, September 2006.
  - <sup>4</sup> Mokuno, M., Kawano, I., Suzuki, T., "In-Orbit Demonstration of Rendezvous Laser Radar for Unmanned Autonomous Rendezvous Docking" IEEE Transactions On Aerospace And Electronic Systems Vol. 40, No. 2 April 2004.
  - <sup>5</sup> Pronk, Z. and van Woerkom, P.Th.L.M. "Flat-Floor Facilities in Support of Configurable Space Structures Development." Acta Astronautica, Vol. 38, Nos. 4-8, pp. 277-288, 1996.
  - <sup>6</sup> Pavlich, J., Tchoryk, P., Hays, A., Wassick, G. "Kc-135 Zero G Testing Of A Micro Satellite Docking Mechanism" Space Systems Technology and Operations, Proceedings of SPIE Vol. 5088, 2003
  - <sup>7</sup> Otero, A.S., Chen, A., Miller, D.W., Hilstad, M. "SPHERES: Development of an ISS Laboratory for Formation Flight and Docking Research." 0-7803-7231-X/01, IEEE, 2002.
  - <sup>8</sup> Barnhart, D., Barret, T., Sachs, J., Will, P. "Development and Operation of a Micro-Satellite Dynamic Test Facility for Distributed Flight Operations" AIAA Space 2009, September 2009
  - <sup>9</sup> Everist, J., Mogharei, K., et al. "A System for In-Space Assembly." Proceedings of IEEE/RSJ International Conference on Intelligent Robots and Systems, 2004
  - <sup>10</sup> Barnhart, D., "Developing the Future of Orbital Assembly: Discoveries and Demonstrations of Critical Technical Needs for Autonomous Robotic Assembly in Space", SERC/ISI White Paper, SERC-09-003, July 1 2009.
  - <sup>11</sup> Balch, T., Arkin, R.C. "Behaviour-based Formation Control for Multi-robot Teams" IEEE Transactions on Robotics and Automation, 1999.
  - <sup>12</sup> DeMenthon, D.F. and Davis, L.S., "Model Based Object Pose in 25 Lines of Code"
  - <sup>13</sup> Wertz, J.A., Lee, A.Y. "In-flight Estimation of the Cassini Spacecraft's Inertia Tensor"